Supplementary Data

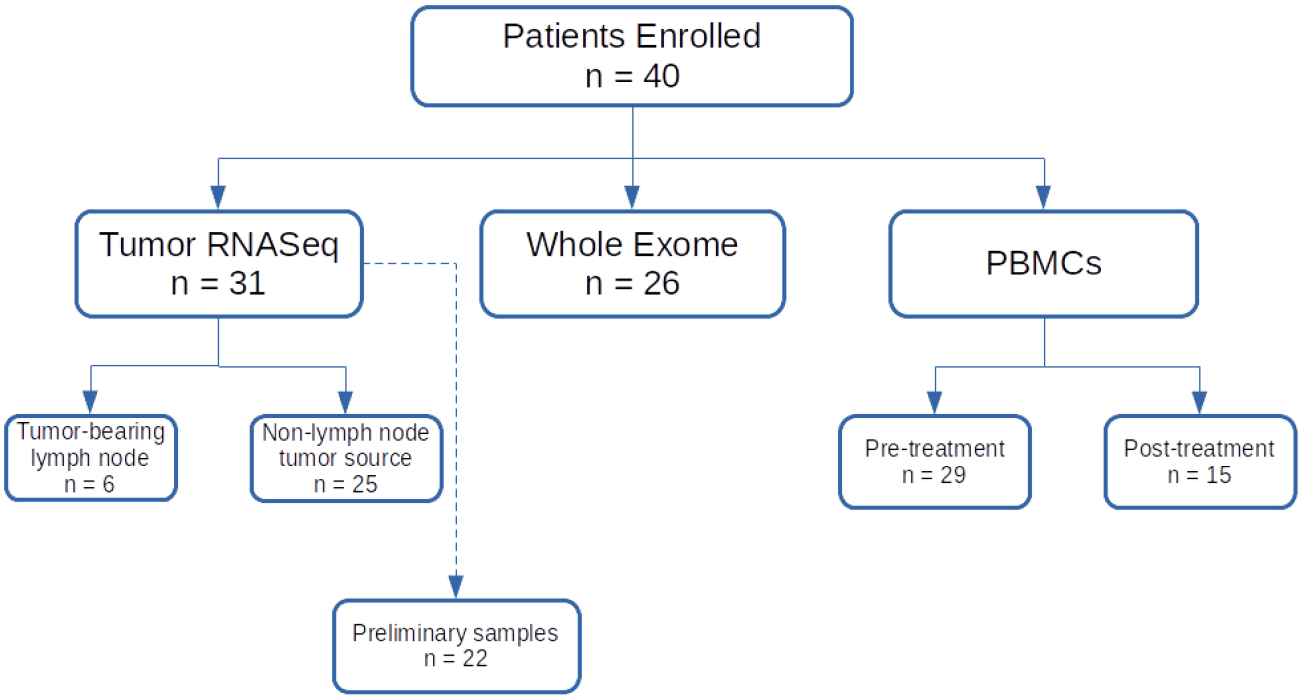

Supplementary Figure 1: Study sample collection counts.

Samples listed by data type, optionally further divided by collection time point or clinical attribute.

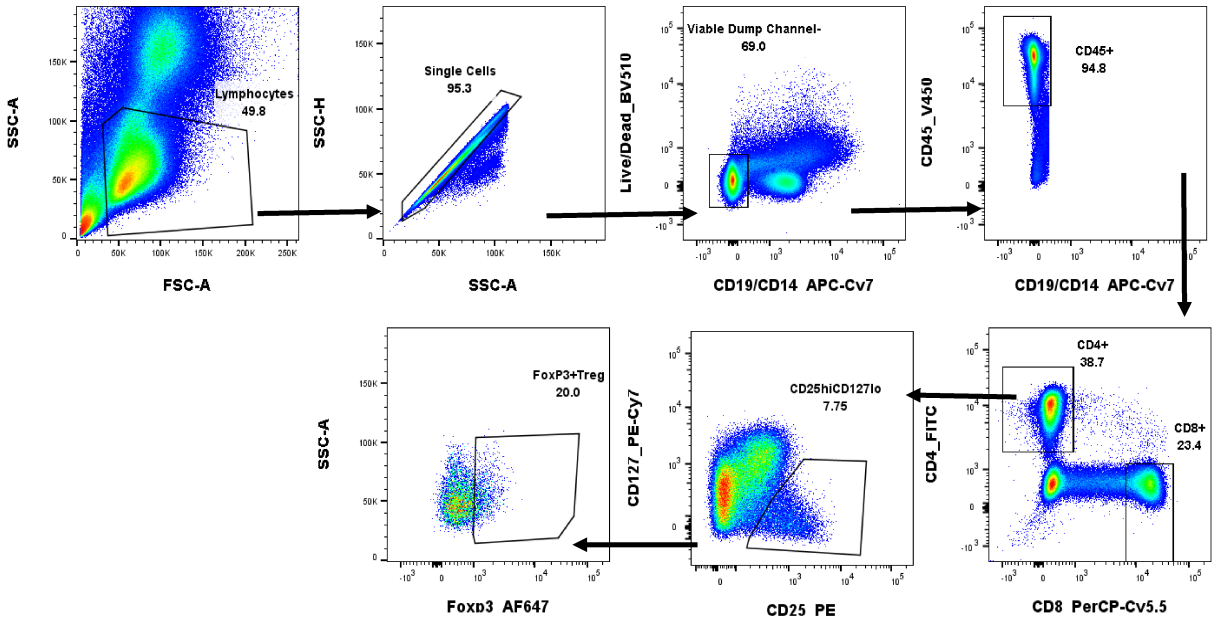

Supplementary Figure 2: Demonstration of gating strategies for T_{reg} flow cytometry analyses.

The first row shows how viable CD45+ PBMCs were selected from a bulk population (from left to right). The second row demonstrates sorting of CD45+ PBMCs into CD4+ and CD8+ T cells, where CD25hiCD127low and FoxP3+ (2nd row) subsets were subsequently detected within CD4+ T cells.

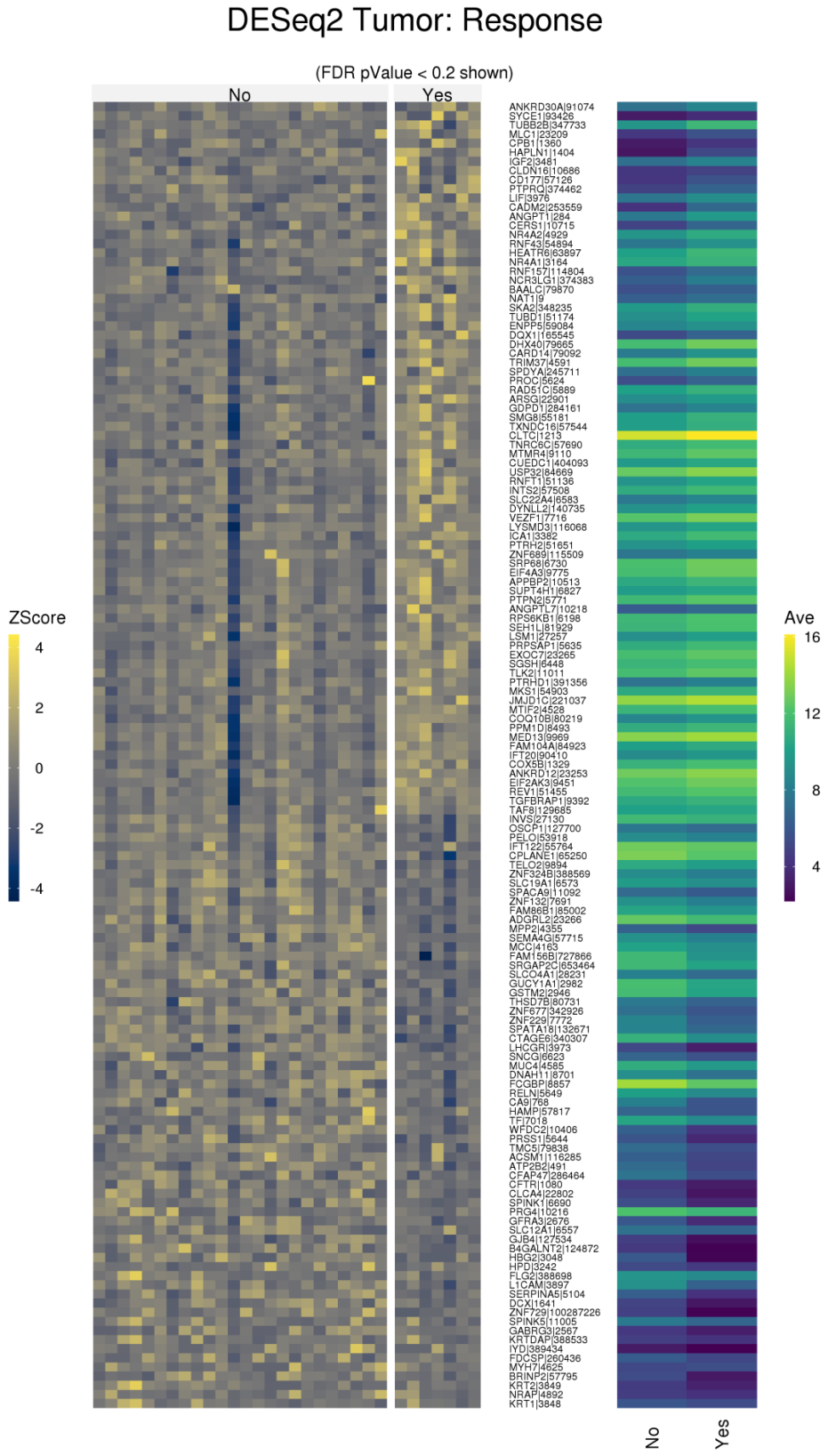

Supplementary Figure 3: Tumor differential gene expression, by response to therapy.

Readable gene names and group averages, to accompany Fig 3C (n=31).

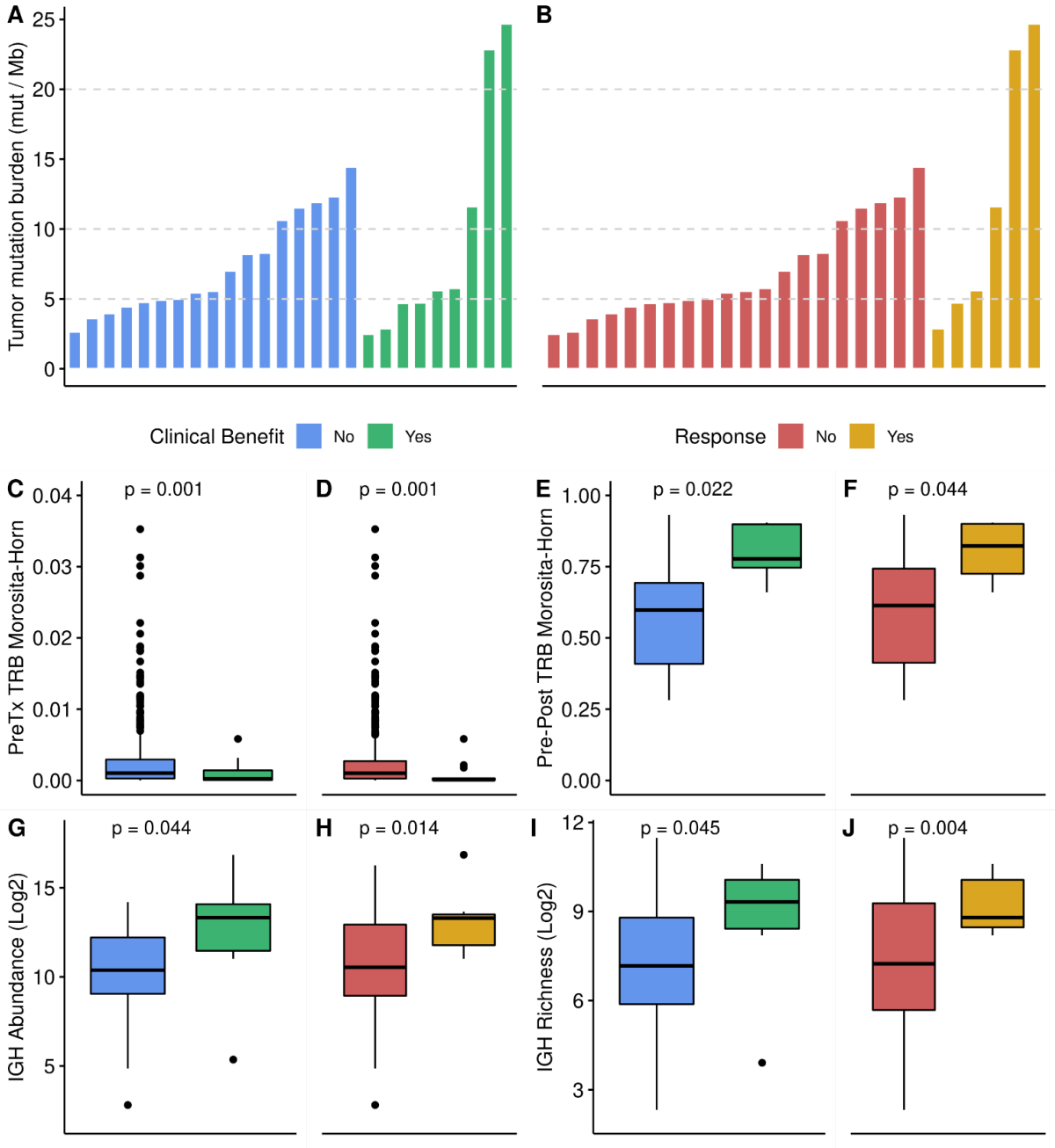

Supplementary Figure 4: Tumor mutation burden and diversity metrics

A-B: TMB did not significantly differ between groups by clinical benefit (A) or response (B) by either stratification (low <10 mut/Mb, high >=10 mut/Mb ; or low: <5 mut/Mb, intermediate: 5-20 mut/Mb, high: >= 20 mut/Mb; Wilcoxon Rank Sum p > 0.29). C-D: Pre-treatment PBMC-derived T-cell beta chain repertoire similarity (n=29) was lower (p<0.05) in intra-group comparisons by either future clinical benefit (C) or response (D). E-F: T-cell beta chain repertoire similarity (n=15) was higher comparing pre and post treatment samples in patients with either clinical benefit (E) or response (F). G-J: Higher IgH chain abundance and richness was associated (p<0.05) with both clinical benefit (G, I) and response (H, J) in tumor RNA-Seq (n=31).

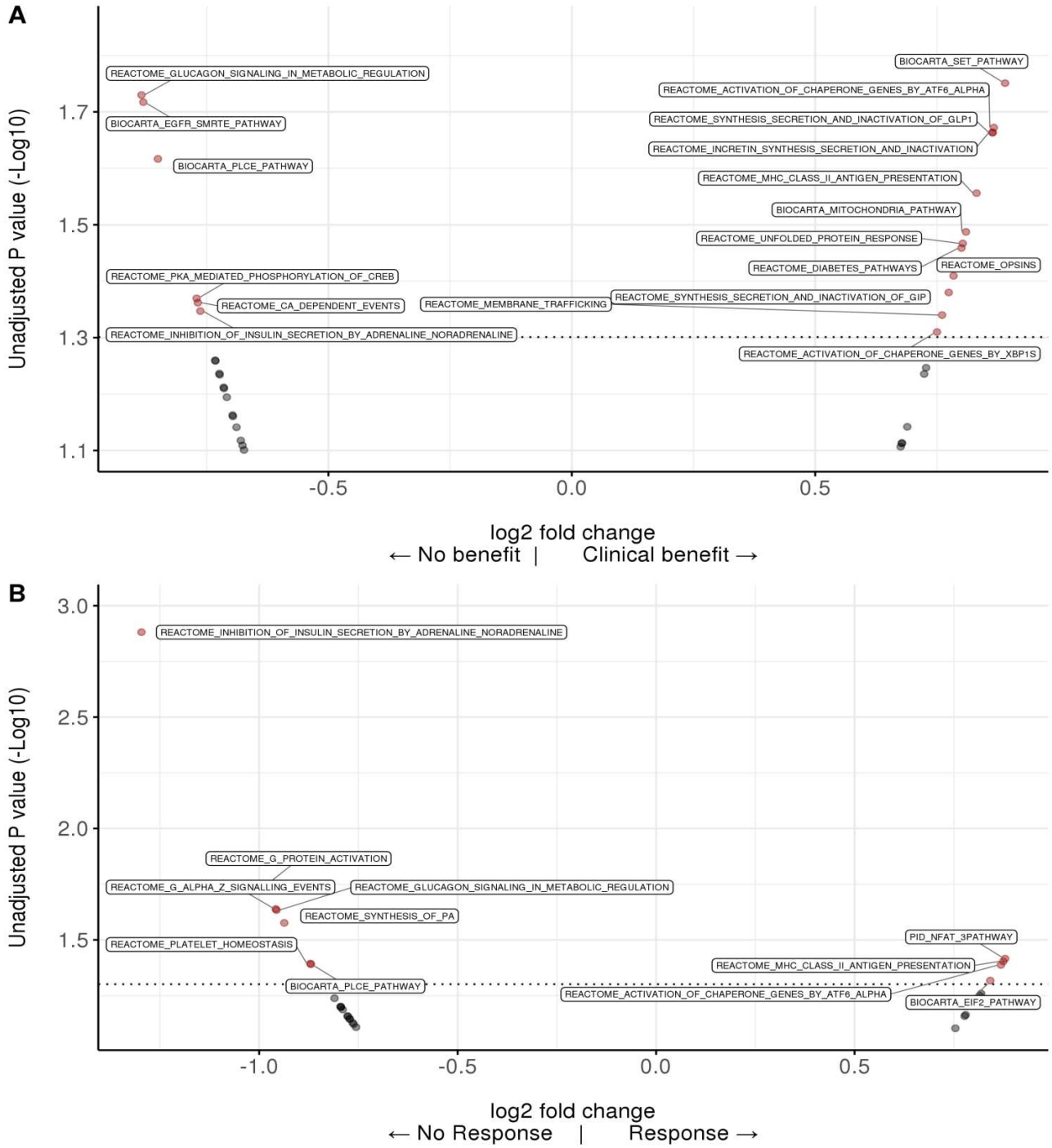

Supplementary Figure 5: Gene set enrichment

No gene sets were significant by FDR testing in all tumor samples (n=31) by either clinical benefit (A) or response (B). Note the p-value scales have been adjusted to make labels visible in this graphic.

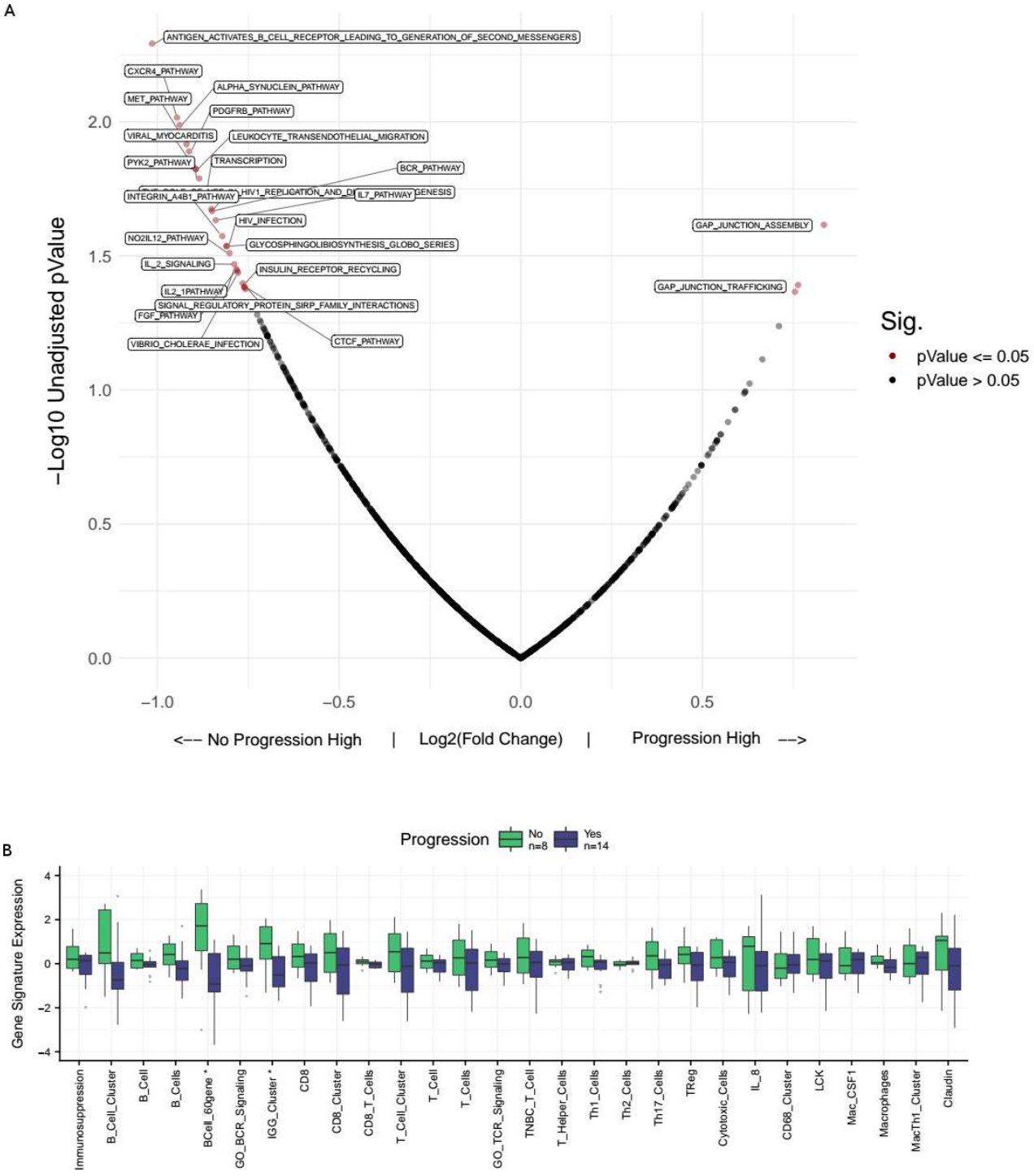

Supplementary Figure 6: Tumor RNASeq Subset Analysis.

Results from a subset of tumor RNASeq samples (n=22). A: Gene set enrichment, B: Immune gene signatures, demonstrating overexpression in B-cell receptor pathways and B-cell signatures in patients without progression of disease.

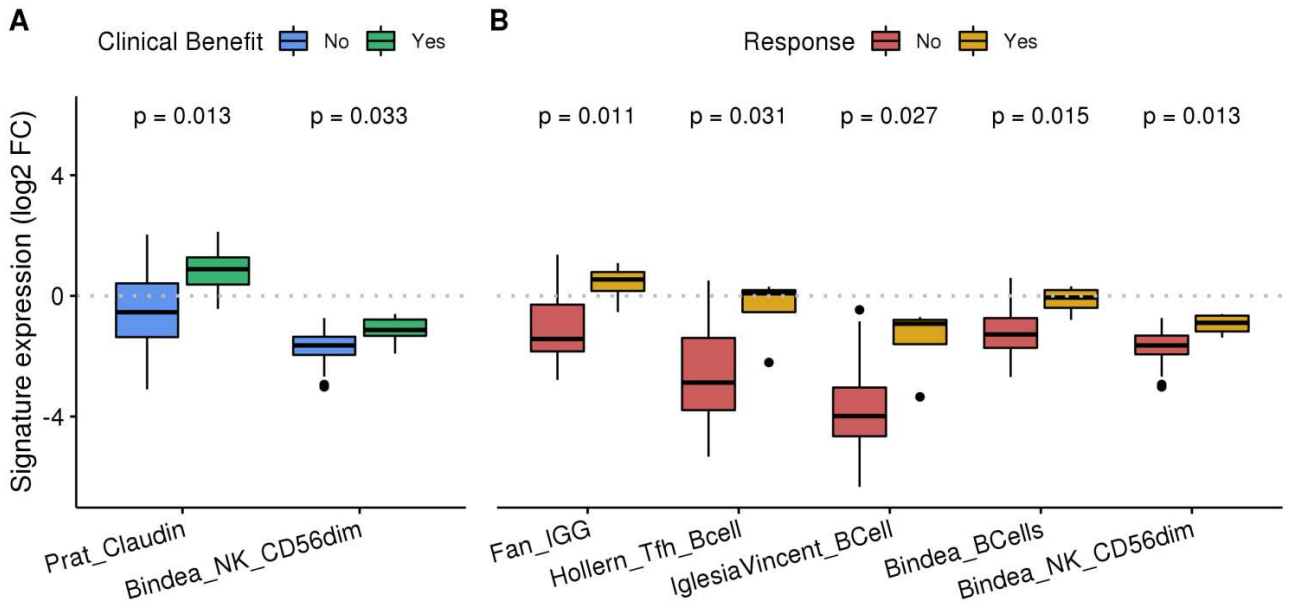

Supplemental Figure 7: Immune gene features in non-nodal tumor samples

A-B: Immune gene signatures associated ($p<0.05$) with clinical benefit (CR+PR+SD; A) and response (CR+PR; B) were enhanced after excluding nodal tissue samples.

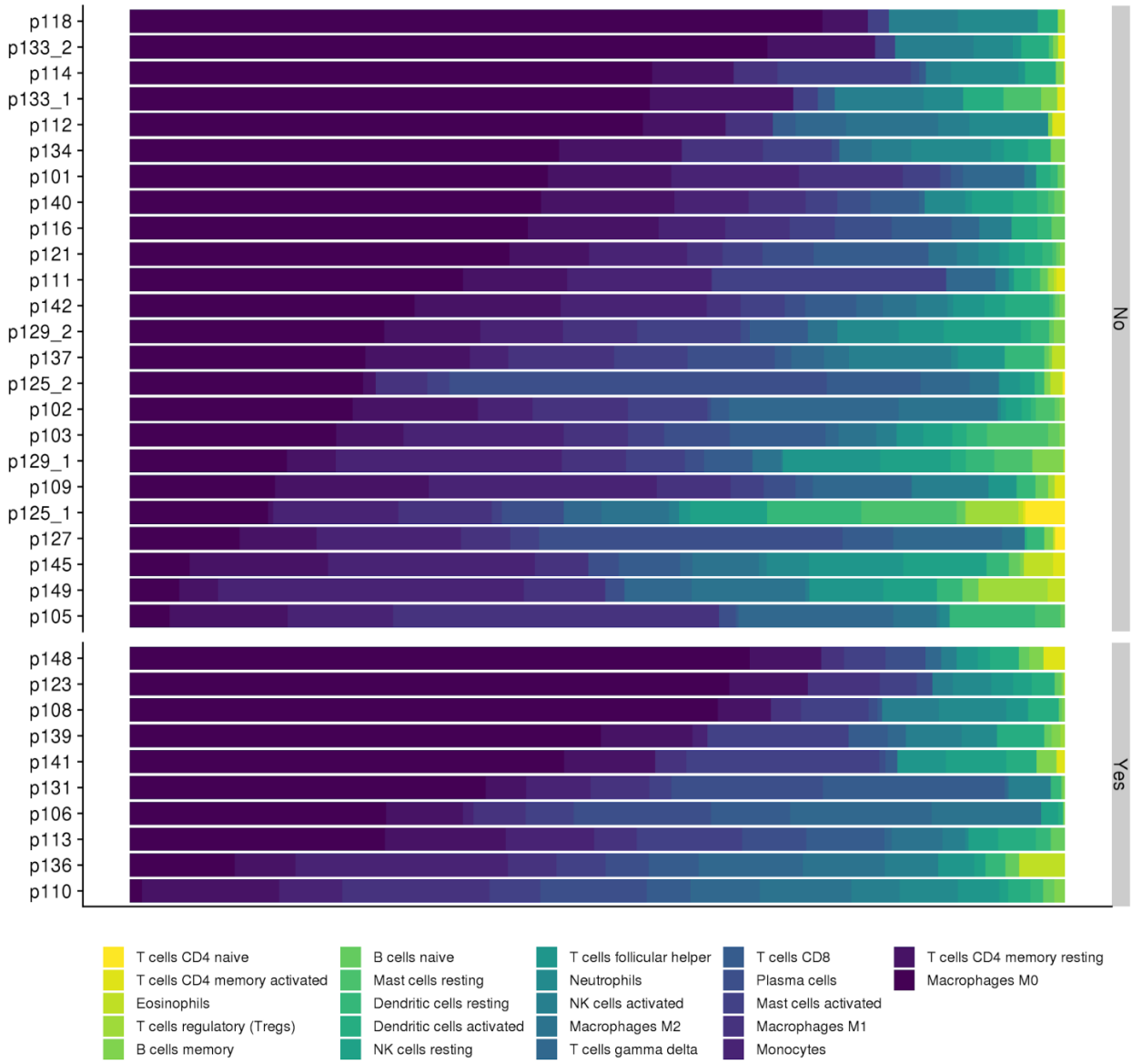

Supplementary Figure 8: Imputed tumor immune cell mixture.

Samples sorted by response status. There were no significant differences in imputed immune cell fractions by response or clinical benefit (two-tailed T-test).

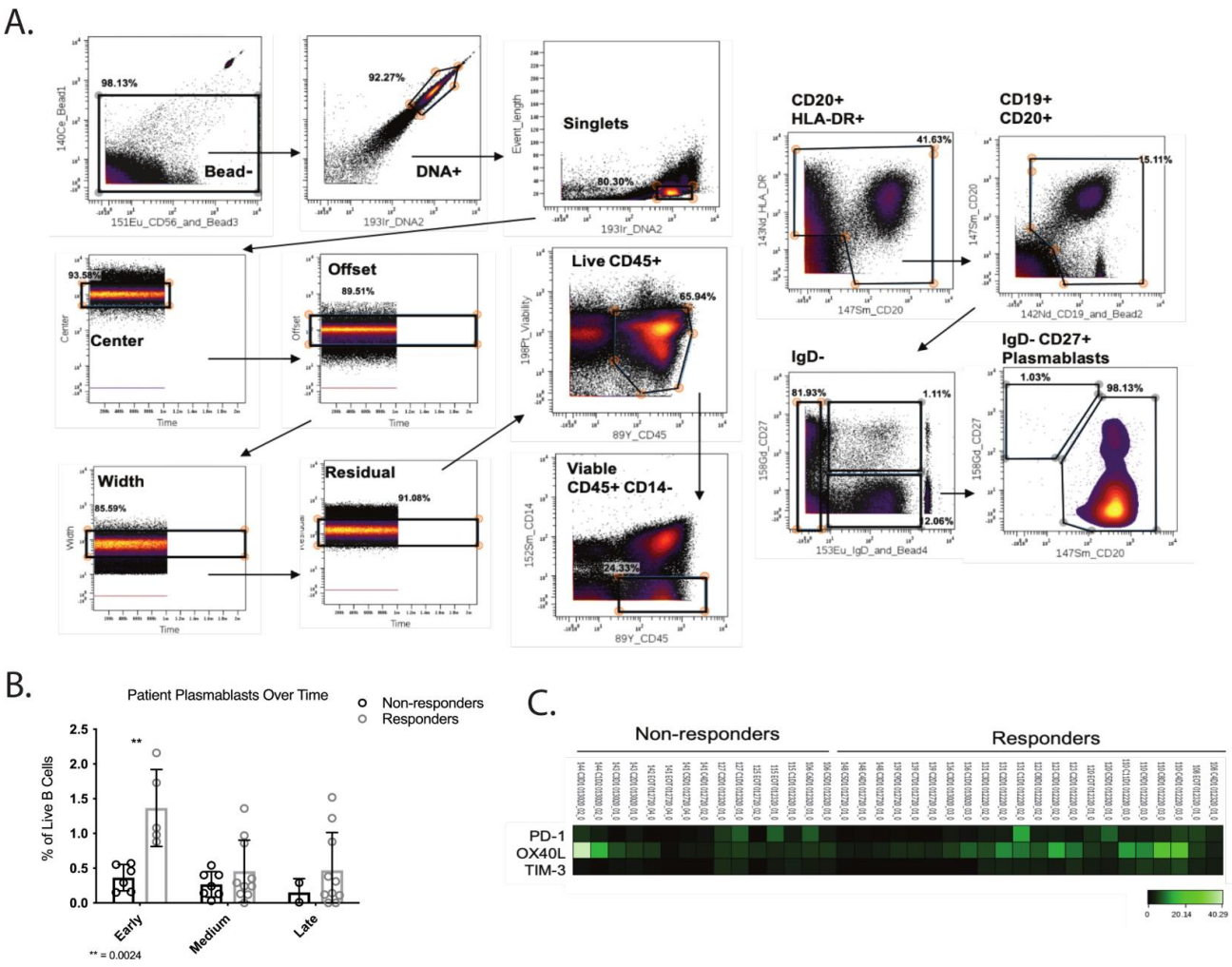

Supplementary Figure 9: CyTOF of peripheral plasmablasts.
Patients whose metastatic TNBC responded to a priming dose of cyclophosphamide prior to pembrolizumab exhibit an increased frequency of plasmablasts in the peripheral blood early during treatment (cycles 1-2). A: Gating strategy used to eliminate metal-spiked beads, doublets, dead cell debris, CD45- cells and CD45+ monocytes. B: The gating strategy described in (A) was further used to identify additional hematopoietic subpopulations of interest, including plasmablasts [HLA-DR (Nd134Di), CD20 (Sm147Di), CD19 (ND124Di), IgD (Eu153Di), and CD27 (Gd158Di)], of peripheral blood plasmablasts in non-responders and responders across early (Cycle 1-2, 6 non-responders, 5 responders), middle (Cycle 3-5, 7 non-responders, 10 responders), or late (Cycle 6+, 2 non-responders, 10 responders) timepoints. An unpaired Student's t-test was used to determine statistical significance, p = 0.0024. C: Heat map assessment of PD-1, OX40L and TIM-3 expression on IgD- CD217- plasmablasts as gated in B

A.

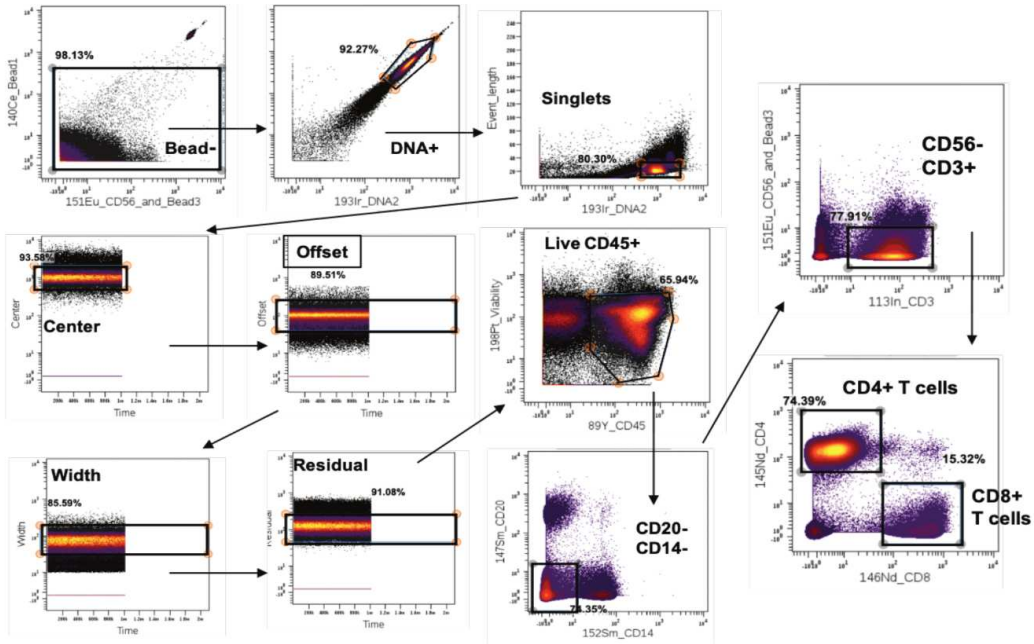
98.13%
Bead-
92.27%
DNA+
Singlets
80.30%
93.58%
Center
Offset
89.51%
Live CD45+
65.94%
CD56-
CD3+
77.91%
Width
85.59%
Residual
91.08%
CD20-
CD14-
CD4+ T cells
74.39%
15.32%
CD8+
T cells

B.

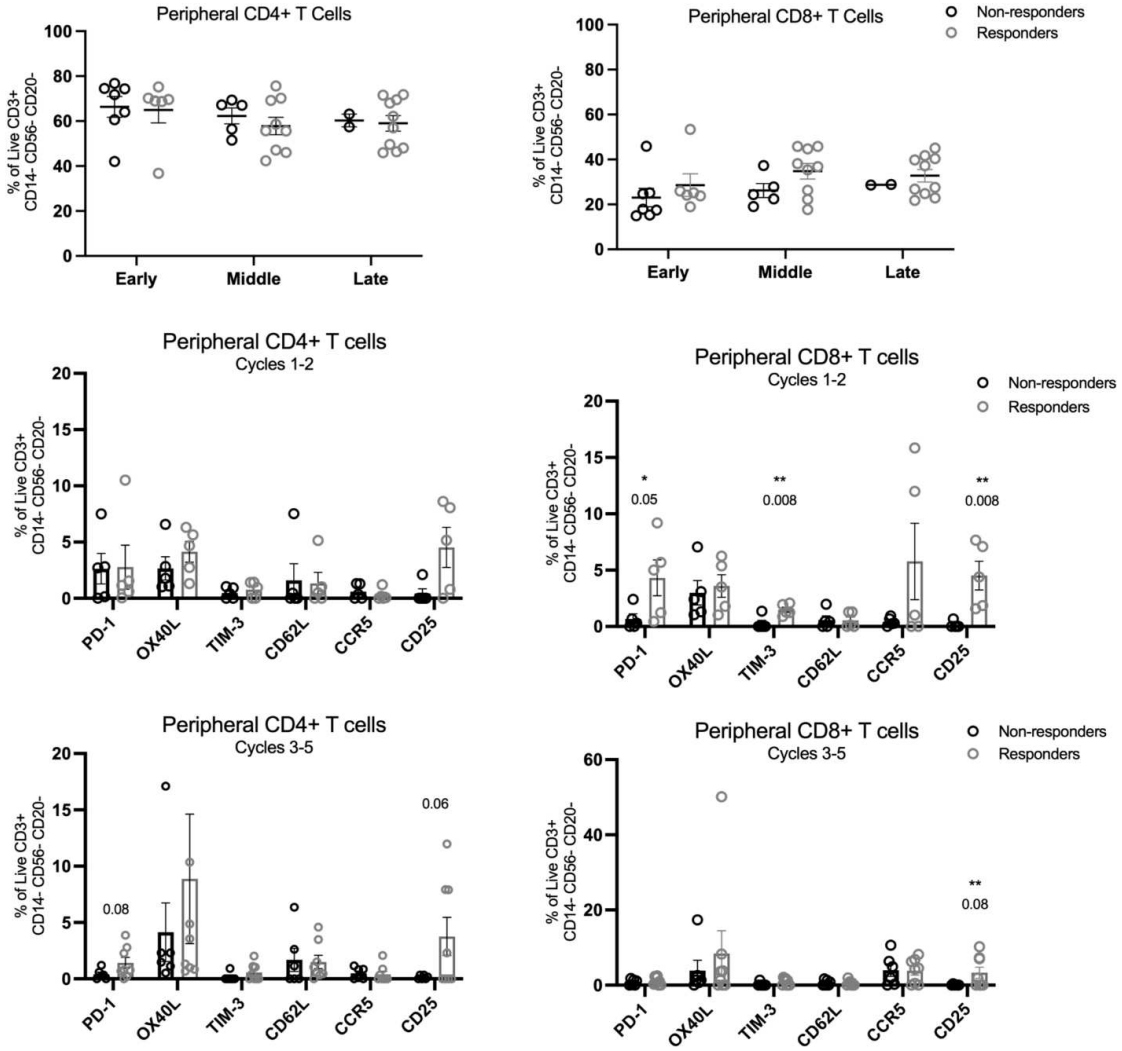
Peripheral CD4+ T Cells
Peripheral CD8+ T Cells
Non-responders
Responders
% of Live CD3+ CD14- CD56- CD20-
Early
Middle
Late
Peripheral CD4+ T cells
Cycles 1-2
Peripheral CD8+ T cells
Cycles 1-2
0.05
0.008
0.008
Peripheral CD4+ T cells
Cycles 3-5
Peripheral CD8+ T cells
Cycles 3-5
0.08
0.06
0.08
PD-1
OX40L
TIM-3
CD62L
CCR5
CD25

Supplementary Figure 10: CyTOF of peripheral T-cell subsets

A: Gating strategy used to eliminate metal-spiked beads, doublets, dead cell debris, CD45- cells, CD20+ / CD14+ monocytes, CD3- and CD4-/CD8- cells. B: The gating strategy described in (A) was further used to identify CD4+ and CD8+ T-cell subsets, shown by treatment timepoint [early (Cycle 1-2, 6 non-responders, 5 responders), middle (Cycle 3-5, 7 non-responders, 10 responders), or late (Cycle 6+, 2 non-responders, 10 responders)] and by expression for early (Cycles 1-2) and middle (Cycles 3-5) timepoints.